Temperature dependence of the Raman linewidth and line shift for the $Q(1)$ and $Q(0)$ transitions in normal and para-H_2

William K. Bischel and Mark J. Dyer
Chemical Physics Laboratory, SRI International, Menlo Park, California 94025
(Received 11 October 1985)

Using stimulated Raman gain spectroscopy, we have measured the temperature and density dependence of the Raman linewidth and line shift for the $Q(1)$ and $Q(0)$ vibrational transitions in H_2 covering the range 77—480 K and 1—20 amagats, and as a function of ortho to para ratio. We conclude that the dominant contribution to the $Q(1)$ linewidth comes from vibrational dephasing collisions, an effect not included in current theories. The line-shift coefficient has a much larger temperature variation than the linewidth coefficient, with the ratio of line shift to linewidth reaching a maximum value of 7.3 at 81 K. These results are important for applications requiring the tuning of the Stokes frequency generated by the stimulated Raman process.

I. INTRODUCTION

The ability to measure the linewidths and line shifts of Raman transitions at high resolution was vastly improved with the demonstration in 1977 of cw and quasi-cw stimulated Raman gain spectroscopy (SRGS)[1] using lasers with linewidths in the tens of MHz. The resolution obtainable for this type of spectroscopy is usually limited by the Doppler width, which in the case of Raman transitions can be extremely small (100 MHz or less). This high resolution provides a unique opportunity for studying the basic physics of the collisions that contribute to the Raman linewidth and line shift.

Important information can be obtained about these collisional processes if the temperature is varied (in addition to the density) since this will change both the relative velocity of the collision and the relative number density of perturbers in a particular rotational state. Calculations of the linewidths and line shifts (see, for example, Ref. 2) can yield information about the intermolecular forces governing the collisional processes. The temperature dependence could also be an important part of the analysis if data were available.

This study was motivated primarily by the following questions: how do the Q-branch Raman linewidths in H_2 vary as a function of temperature, and what collisional mechanisms contribute to the observed density-broadening coefficient? *Ab initio* theories of the Raman linewidth[3,4] predict a large temperature variation for the Q-branch vibrational Raman linewidth, while predicting little variation for the S-branch rotational Raman linewidth. This difference results from the fact that the dominant contribution to the Q-branch linewidths arises from resonant rotationally inelastic collisions, and therefore the linewidth will be a strong function of the relative population in nearby rotational levels. For example, the $Q(1)$ linewidth should depend strongly on the population in the $J=3$ level. This population can be changed by 3 orders of magnitude by changing the temperature from 298 to 77 K. At 77 K, the residual linewidth should reflect the broadening mechanisms that have been left out of current line-broadening theories and thus give new data for theoretical studies.

Several experimental[5–9] determinations of Raman linewidths exist for H_2 at room temperature. Unfortunately, data at other temperatures exist for only a few cases. There has recently been a study of the temperature dependences of the linewidth and line shift for the rotational Raman transitions in H_2.[10] However, as noted above, we expect the rotational Raman linewidths to have a much different temperature dependence, and hence the temperature dependence of the Q-branch linewidths cannot be determined from this study. Linewidth data as a function of temperature for the vibrational Q-branch transitions were obtained in only one experiment[7] over a very limited temperature range. No studies have been made of the linewidth at temperatures below 273 K, probably because the Raman linewidth is very narrow for Q-branch transitions and thus it is only since the recent development of SRGS that high-resolution experiments have been possible.

The determination of the Raman line shift as a function of density and temperature is also important because the collisional mechanisms that contribute to the line shift are different from those contributing to the broadening. The line shift has received much less attention theoretically than the linewidth, probably because of the lack of precise data. There are only two early studies of the Q-branch line shift as a function of temperature.[7,11] We concluded that both the linewidth and line shift need to be determined to provide high quality data for a broad range of temperatures for continued development of the theory.

This research was also motivated by the recent revival of the technique of stimulated Raman scattering, primarily in H_2, as a method of laser frequency conversion. This revival is largely due to the development of high-power, efficient excimer lasers that can serve as the pump source for many applications. One important application is the frequency conversion of the XeF and XeCl lasers to the blue-green[12] frequencies for naval communications. Other applications for excimer lasers include techniques for aperture combining[13] and beam cleanup.[14] All these ap-

plications require that the Raman linewidth in H_2 be accurately known as a function of temperature as well as density.

A second application is the conversion of lasers to the ultraviolet (uv)[15,16] and vacuum ultraviolet (vuv)[17] frequencies using the anti-Stokes lines produced by multiwave mixing in H_2. One group[16] observed a marked increase in the uv conversion efficiency when the temperature was reduced from 298 to 77 K and qualitatively explained their data as resulting from a temperature-induced change in the Raman linewidth. The temperature dependence of the Raman linewidth is an important parameter in the theoretical analysis of this frequency conversion process[18] and needs to be accurately determined.

We therefore started a research program designed to study this interesting problem, and we report here the first experimental results. Preliminary results of these experiments have been reported earlier.[19]

II. EXPERIMENTAL

The SRGS experimental apparatus, illustrated in Fig. 1, is basically similar to the one described by Owyoung.[1] The experiment involves two cw lasers, one operating as the probe laser at the Stokes frequency and one operating as the pump laser. The probe laser is a single-frequency argon-ion laser tuned to 488 nm. The frequency of this laser system was determined to drift less than 10 MHz during the course of an experimental scan. The pump laser is an electronically tunable single-frequency Coherent Model No. 699-21 ring dye laser operating at 612 nm for the experiments on the $Q(1)$ transition. The time-integrated linewidth of this laser system is quoted by the manufacturer to be less than 1 MHz. The pump laser is amplitude modulated at 100 kHz with a electro-optic modulator, combined with the probe laser on a dichroic mirror, and mode matched into a multipass Raman cell.

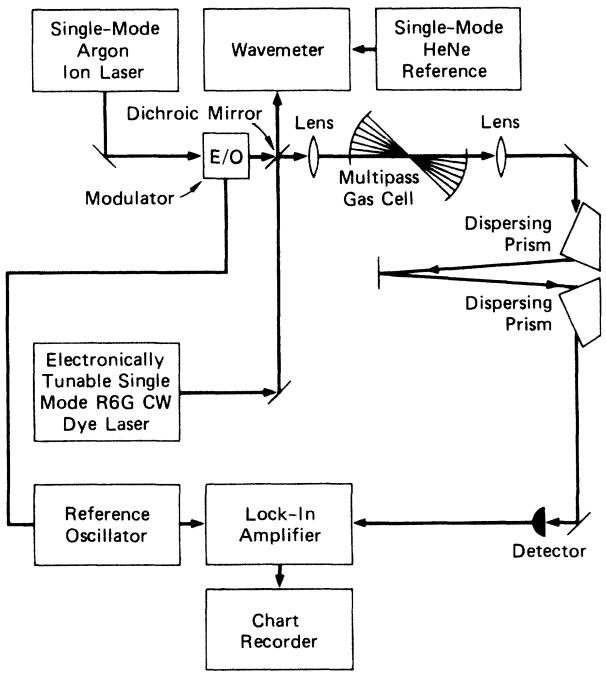

FIG. 1. Experimental configuration used for the cw stimulated Raman gain spectroscopy in H_2.

The multipass cell is the heart of the experiment. Similar multipass cells have been used in other experiments.[1,20] The multipass optics consists of two mirrors with a 30 cm concave radius spaced approximately 60 cm apart. The lasers enter and exit the multipass cell through small holes in the mirror substrates. We have designed and successfully used these optics with both cw and pulsed lasers with up to 50 passes through the Raman cell.

The Raman cell is the product of several design iterations to achieve the requirements of simultaneously obtaining a broad temperature operating range coupled with high-pressure operation. The windows on the cell are AR-coated sapphire that has been braised into a special conflat flange designed to cover the temperature range of 77—500 K at pressures of up to 500 psi. The entire system, including the multipass optics and the Raman cell, is then mounted in a vacuum enclosure to minimize beam-steering effects and condensation on the windows as the cell temperature is changed.

After the lasers exit the multipass cell, the pump and Stokes lasers are focused into a double-pass Raman cell that serves as a reference cell for the line-shift experiments. In this cell the temperature is held constant at 298 K while the density is varied over a limited range, depending on the temperature and density of the multipass cell.

After exiting the double-pass reference cell, the probe laser is separated from the pump laser, using a pair of dispersing Pellin-Broca prisms, and is detected by a fast photodiode. As the pump laser is electronically scanned through the Raman resonance, it acquires a 100-kHz modulation through the Raman gain process. This modulation forms the observed signal. The signal is extracted from the noise with a lock-in amplifier that has been referenced to the 100-kHz modulation and is recorded using an x-y plotter.

The accurate measurement of pressure-induced Raman line shifts presents a difficult problem because the conventional technique requires that both narrow-band laser systems be actively stabilized to high precision. We eliminated this problem in our experiment by including the double-pass room-temperature reference Raman cell (not shown in Fig. 1) after the variable-temperature Raman cell. The recorded Raman gain signal was therefore a combination of two signals that were deconvolved from each other in the data-fitting procedure. In this manner we obtained the line-broadening and shift data relative to room-temperature data during the same scan of the dye laser.

The pressure in the experimental cells was measured using a 10 000-torr MKS Baratron gauge, and the temperature was measured using a Chromel-Alumel thermocouple gauge referenced to 273 K. The density was calculated using the perfect-gas law since the density calculated using the second virial coefficient[21] deviates from this calculation by less than 1% at the maximum density of 12 amagats used in these experiments.

Para-H_2 was generated by storing gas evaporated from

liquid H_2 in an aluminum cylinder. Tests of the para-ortho conversion rate using spontaneous Raman scattering indicated that the percentage of para-H_2 did not change during the experiment.

III. RESULTS

An example of typical experimental data for the $Q(1)$ transition in H_2 at 81 K is given in Fig. 2. Here we see two well-spaced resonances with slightly different widths, one from the room-temperature reference cell and one from the cooled Raman cell. We note that the line shift is significantly larger than the line broadening at this temperature. From data taken at many temperatures and densities, we can derive the temperature dependence of the linewidth and line shift.

A. Linewidth analysis

A Lorentzian line-shape function was used to determine the full width at half maximum (FWHM) Raman linewidth from the Raman gain signals. The line shapes are theoretically predicted to have Lorentzian profiles. Within the limit imposed by our signal-to-noise ratio, we observed no deviation from the Lorentzian line shape at the lowest densities used in this experiment (0.93 amagats). The FWHM linewidths were plotted as a function of density at each temperature.

Figure 3 gives an example of the linewidth data for the $Q(1)$ transition at 81, 298, and 474 K. The data at 298 and 81 K were taken on several different days over about a year. Thus the resulting scatter represents the internal consistency of the experiment. We can see from Fig. 3 that this consistency is very good, particularly since the electronic scan drive for the dye laser was recalibrated many times during that year.

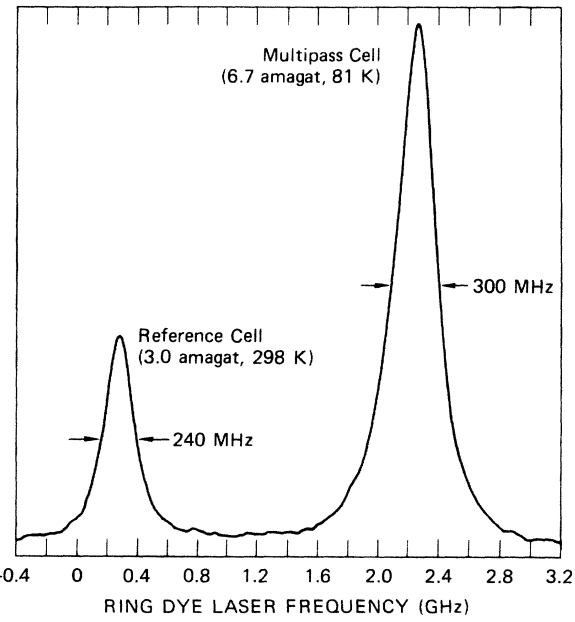

FIG. 2. Raman gain signal at 81 K, illustrating the linewidth and line shift of the $Q(1)$ Raman line in H_2. At this temperature the shift coefficient is 7.3 times larger than the broadening coefficient. Zero on the frequency scale is the zero-density position of the Raman line at 4155.25 cm^{-1}.

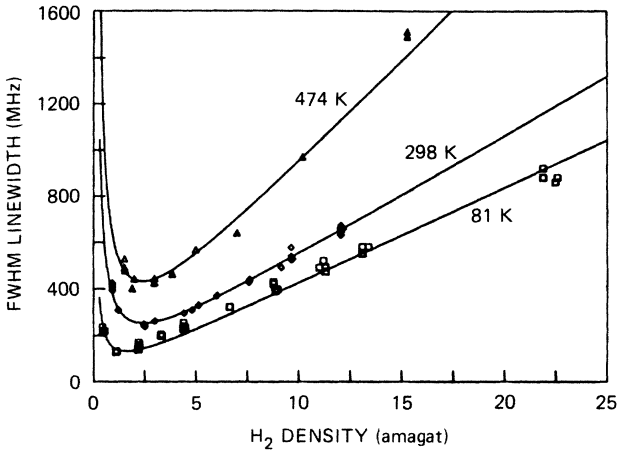

FIG. 3. Density dependence of the experimental FWHM Raman linewidths (MHz) at temperatures of 81, 298, and 474 K. The solid lines are fits to Eq. (1), yielding the A and B coefficients given in Table I.

The solid lines in Fig. 3 are the least-squares fits to the linewidths using the diffusion model (Dicke narrowing) described in Sec. IV. The fitting formula for the FWHM linewidth is of the form

$$\Delta\nu_{\mathrm{FWHM}} = A/\rho + B\rho \,, \tag{1}$$

where A is a coefficient proportional to the self-diffusion coefficient, ρ is density, and B is the density-broadening coefficient. The coefficients A and B at each temperature were then derived from these fits and are the final result of the data analysis, as listed in Table I.

Figure 4 gives the temperature dependence of the

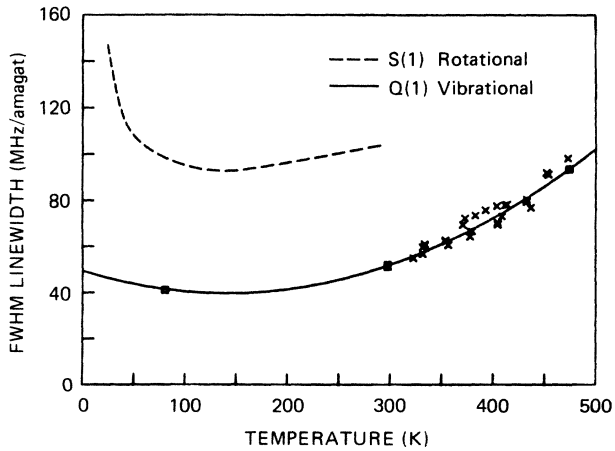

FIG. 4. Temperature dependence of the Raman linewidth for the $Q(1)$ vibrational transition in H_2. The squares are data taken at 81, 298, and 474 K, and the $\times$'s are individual measurements at other temperatures. The triangle is the data of Owyoung (Ref. 9). The solid line is the fit to the data given by Eq. (2). The dotted line is the data of van den Hout *et al.* (Ref. 10) for the $S(1)$ rotational Raman line.

TABLE I. Temperature dependence of the $Q(J)$ Raman linewidth parameter.

			A (MHz amagat)		B (MHz/amagat)	
T (K)	J	$R_{o\text{-}p}$	This work	Previous work	This work	Previous work
81	0	3:1	189±40		29.0±1.0	
	0	1:7.7	76± 6		45.4±0.8	
	1	3:1	107±20		41.5±0.6	
298	0	3:1	257±12		76.6±0.8	66.0±5.0[a] 70[b] 83.0±3.0[c]
	1	3:1	309±11	302±9[d]	52.2±0.5	51.3±0.6[d] 45.0±3[a] 42[b] 55.0±2.0[c] 53.1[e] 63[f]
474	1	3:1	508±29		94.0±2.0	

[a]Reference 22.
[b]Reference 6.
[c]Reference 8.
[d]Reference 9.
[e]Reference 5.
[f]Reference 7.

density-broadening coefficient B in Eq. (1) for the Raman linewidth of the $Q(1)$ transition. The data taken at 81, 298, and 474 K are indicated by the squares. The values for A and B determined from Eq. (1) are also given in Table I. Data taken at other temperatures are indicated by the $\times$'s in Fig. 4. These measurements are much less accurate than those at the above three temperatures but they show the consistency of the measurement. In the study of the $Q(1)$ linewidth, the ortho-para ratio ($R_{o\text{-}p}$) was not varied.

Table I also lists the results of previous measurements of the $Q(1)$ linewidth at 295 K by Owyoung,[9] Murray and Javan,[22] Allin *et al.*,[6] Hunt *et al.*,[8] and Foltz *et al.*[5] We observe that our measurements agree almost exactly with the data of Owyoung,[9] who used the SRGS technique, whereas those measurements of the other authors differ by 15–20%. We believe that the current value is correct to better than 5% due to the high resolution afforded by our experimental technique. The only other set of linewidth data in the literature for the $Q(1)$ transition is that of Lallemand and Simova.[7] Although they reported temperature measurements over a limited range with the same qualitative trend as our data, their linewidths are 30% larger than ours. This discrepancy probably results from the inherent difficulties of running a single-mode laser coupled with a stimulated Raman experiment.

Figure 4 also plots (dashed line) the rotational Raman linewidth for the $S(1)$ transition determined by van den Hout *et al.*[10] We note that the broadening coefficient is a factor of 2 larger than the $Q(1)$ transition at 298 K and has little temperature dependence. As will be discussed in Sec. IV, the rotational Raman lines are expected to have larger linewidths.

The solid line in the figure is a phenomenological second-order fit to the $Q(1)$ linewidth. When we include both terms in Eq. (1) to model the Raman linewidth at any density, we derive a best-fit formula for the FWHM Raman linewidth in MHz for temperatures between 77–500 K, densities of 1–50 amagats, and for an ortho-para ratio of 3:1 as

$$\Delta\nu(\rho)=\frac{309}{\rho}\left[\frac{T}{298}\right]^{0.92} +[51.8+0.152(T-298) +4.85\times10^{-4}(T-298)^2]\rho\ . \quad (2)$$

Here $\Delta\nu$ is the FWHM Raman linewidth in MHz, ρ is the density in amagats, and T is the temperature in K. This phenomenological fit could be improved if data were taken at temperatures between 81 and 298 K.

Data for the $Q(0)$ transition in H_2 were acquired at temperatures of 298 and 81 K for an ortho-para ratio ($R_{o\text{-}p}$) of 3:1, and at 81 K for ortho-para ratios of 3:1 and 1:7.7. A and B values derived by fitting the data to Eq. (1) are given in Table I. The signal-to-noise ratios for the $Q(0)$ data were somewhat worse than the $Q(1)$ data shown in Fig. 2. This limited the parameter space that could be investigated with the experimental apparatus. Improved signal-to-noise ratios could be obtained using the recently developed modulation techniques of Rosasco *et al.*[23] with a modification of our signal-detection apparatus. We hope to modify our experiment in the future to allow $Q(0)$ data to be obtained at lower densities and for different ortho-para ratios.

B. Line-shift analysis

The line shifts of the $Q(1)$ and $Q(0)$ transitions were measured for each of the temperature and density conditions described above for the linewidth measurements.

Two techniques were used. In the early phase of the experiment, we measured the center frequency of the Raman transition for two successive scans at different densities and then plotted the difference as a function of density. This method assumed that the dye- or argon-laser frequency did not drift during the two scans. This technique yielded data with some scatter because of the uncertainty in the frequencies of the lasers. Later in the experiment, the double-cell approach (described in Sec. II) was implemented with excellent results. The data for the $Q(1)$ transition at 81, 298, and 474 K and the $Q(0)$ transition at 81 K in para-H_2 were taken with the two-cell technique; $Q(1)$ line shifts at other temperatures and the $Q(0)$ line shifts were determined using the first technique.

The Raman line shift can be modeled using a second-order expansion in the density as[11,22]

$$\nu_R(\rho)=\nu_R(0)+C\rho+D\rho^2 , \tag{3}$$

where $\nu_R(0)$ is the zero-pressure Raman transition frequency, and C and D are coefficients that only depend on temperature. Most previous experiments had to operate at such high densities that the term proportional to the density squared had to be included in the data analysis. In our experiments, we were able to operate at densities of less than 25 amagats, and thus a linear fit determining only C in Eq. (3) was used in our data analysis. Only at 474 K was the linear component in Eq. (3) small enough that we had to include the second-order term in the data analysis. The line-shift coefficients (C) for all the transitions, temperatures, and ortho-para ratios investigated are given in Table II. Also given is a comparison with the data obtained by other groups.[7,11,22] The agreement between all the measurements is quite good.

Figure 5 plots the temperature dependence of the linear line-shift parameter for the $Q(1)$ transition for the ortho-para ratio of 3:1 and the temperature range of 77–480 K. The $\times$'s indicate the data taken with the first technique, and the squares indicate data taken with the reference cell technique. The solid line is a phenomenological fit to the data yielding C in MHz/amagat as

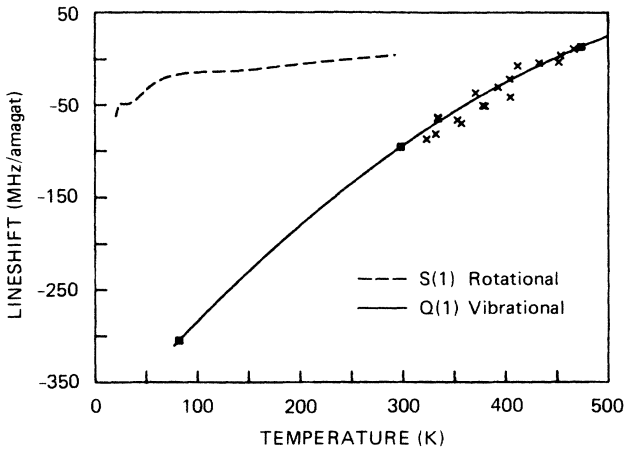

FIG. 5. Temperature dependence of the Raman line shift for the $Q(1)$ vibrational transition in H_2. The squares are data taken at 81, 298, and 474 K, and the $\times$'s are individual measurements taken at other temperatures. The solid line is the phenomenological fit to the data given by Eq. (3). The dotted line is the data of van den Hout *et al.* (Ref. 10) for the $S(1)$ rotational Raman line.

$$\begin{aligned} C&=[\nu_R(\rho)-\nu_R(0)]\rho^{-1} \\ &=[-96.1+0.777(T-298) \\ &\quad -8.82\times10^{-4}(T-298)^2] , \end{aligned} \tag{4}$$

where $\nu_R(0)$ is the zero-density Raman frequency (not measured in this experiment). Also plotted in Fig. 5 by the dashed line is the temperature dependence of the $S(1)$ rotational Raman transition observed in Ref. 10. Note the considerable difference in the temperature behavior of the line-shift parameters for two transitions.

It is surprising to find that the value of $\nu_R(0)$ is not known to better than ±0.02 cm^{-1}. Stoicheff[24] obtained 4155.207 cm^{-1} [extrapolated to zero density using Eq. (4)], Foltz *et al.*[5] obtained 4155.259 cm^{-1}, and Brannon *et al.*[25] obtained 4155.240$\pm$0.02 cm^{-1}. There is a similar uncertainty in the value of the $Q(0)$ transition frequency.

TABLE II. Temperature dependence of the $Q(J)$ Raman line-shift coefficients.

			C (MHz/amagat)		D (MHz/amagat^2)	
T (K)	J	$R_{o\text{-}p}$	This work	Previous work	This work	Previous work
81	0	3:1	-250 ± 10	-270 ± 10[a]		0.16 ± 0.02[a]
	0	1:7.7	-336 ± 10			
	1	3:1	-305 ± 10	-290 ± 10[a]		0.16 ± 0.02[a]
298	0	3:1	-64 ± 5	-71 ± 5[a]		0.168[a]
				-65[b]		0.174[b]
	1	3:1	-96 ± 1	-94 ± 5[a]		0.147[a]
				-90[b]		0.135[b]
				-90 ± 3[c]		
474	1	3:1	9.5 ± 0.9	3.9[c]	0.51 ± 0.07	

[a]Reference 11.
[b]Reference 22.
[c]Reference 7.

This uncertainty could be considerably reduced using the SRGS technique combined with the recently developed wavemeters that have accuracies of a few parts in 10^{-7}.

This plot, coupled with Eq. (4), is important for applications where the Raman frequency needs to be tuned in stimulated Raman frequency conversion. It is interesting that the transition can be tuned in both directions by changing the temperature of the gas. The largest tuning is obtained at 81 K. The ratio of the shift coefficient, given by Eq. (3), to the broadening coefficient, given by Eq. (2), reaches a maximum value of 7.3 at 77 K. This is a very surprising result since this ratio for absorption transitions in the infrared is typically 0.1 or less.

IV. DISCUSSION

The Raman linewidth has a complex density dependence that will change as a function of temperature. To illustrate this dependence, we have plotted in Fig. 6 the density dependence of the FWHM Raman linewidth in the reduced variables of $Y=\Delta\nu_{\mathrm{FWHM}}/\Delta\nu_D$ and $X=\Delta\nu_D\rho/A$, where $\Delta\nu_D$ is the Doppler width and A is proportional to the self-diffusion constant, Eq. (1). The Raman linewidth for all temperatures and densities can thus be represented by one plot.

We can identify three general density ranges in Fig. 6 where different collisional mechanisms play dominant roles. In the low-density region, collisions have little effect on the line shape and the linewidth is determined by Doppler broadening. In this limit, the line shape is a Gaussian with a FWHM linewidth (in Hz) given by

$$\Delta\nu_D=\frac{k_e}{\pi}[2(\ln 2)kT/m]^{1/2}\,, \tag{5}$$

where T is the temperature in K, m is the mass, k is Boltzmann's constant, and k_e is the effective wave vector (angular units) given by[22]

$$k_e=2\pi[2\nu_p\nu_S(1-\cos\theta)+\nu_R^2]^{1/2}\,. \tag{6}$$

Here ν_p and ν_S are the pump and Stokes laser frequencies in cm^{-1}, θ is the angle between the pump and Stokes lasers, and ν_R is the Raman transition frequency (cm^{-1}).[4] For forward scattering ($\theta=0°$), $k_e=2\pi\nu_R$. The Doppler widths for forward scattering for each of the temperatures illustrated in Fig. 3 are given in Table III. We note from Eq. (5) that the Raman linewidth at low density is proportional to $T^{1/2}$.

As the density increases, collisions start to contribute to the line shape. If the most frequent collisional process is elastic velocity-changing collisions, as in the case of H_2, the line shape starts to narrow when the mean free path for collisions is approximately equal to $1/k_e$. This narrowing was first explained by Dicke.[26] A simple physical picture explaining this effect has been given by Murray and Javan.[22]

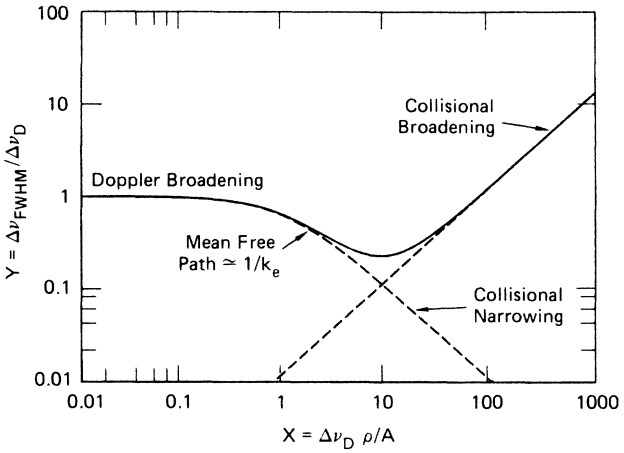

FIG. 6. Density dependence of the Raman linewidth as a function of reduced variables X, Y. The collisional narrowing has been calculated from the hard-collision model (see Ref. 22). In reduced variables, the collisional broadening contribution to the linewidth can be calculated from $Y=X(AB/\Delta\nu_D^2)$, where A and B are given in Table I, and $\Delta\nu_D$ is given by Eq. (5). We have illustrated here the broadening contribution at 298 K for the $Q(1)$ transition.

For densities above 1 amagat, the collisionally narrowed Doppler line shape is Lorentzian and has a FWHM linewidth (in Hz) inversely proportional to density given by

$$\Delta\nu_{\mathrm{FWHM}}=\frac{D_0k_e^2}{\pi\rho}\,, \tag{7}$$

where D_0 is the self-diffusion coefficient in $\mathrm{cm}^2\,\mathrm{amagat}\,\mathrm{s}^{-1}$ and ρ is the density in amagats. This is known as the diffusion model and it has been discussed by several authors.[22,27–29] Unfortunately, this model does not give the correct limit at zero density.

There are several line-shape theories covering the density range between 0 and 1 amagat (Refs. 27 and 28) that predict collisional narrowing and give the proper asymptotic limits. Two types of collisions are considered: the

TABLE III. Temperature dependence of the cutoff density ρ_c for the diffusion model.

T	$Q(J)$	$R_{\mathrm{o\text{-}p}}$	$\Delta\nu_D$ (MHz)	D_0 ($\mathrm{cm}^2\,\mathrm{amagat}\,\mathrm{s}^{-1}$)	ρ_c (amagat)
81	0	3:1	569	0.871	1.10
	0	1:7.7	569	0.350	0.45
	1	3:1	568	0.493	0.63
298	0	3:1	1090	1.19	0.79
	1	3:1	1089	1.42	0.92
474	1	3:1	1373	2.34	1.23

hard collision, where the mass of the collision partner is larger than the radiator, and the soft collision, where the mass of the collision partner is smaller than the radiator. Although collisions for H_2 lie between these two limits, Murray and Javan[22] have concluded that the hard-collision model best fits their results.

We plot the FWHM linewidth ($\Delta\nu_{\mathrm{FWHM}}$) predicted by the hard-collision model and diffusion model in Fig. 7, where the reduced variables are the same as those used in Fig. 6. At $X=3.33$, the hard-collision model predicts a linewidth that is $\sim 10\%$ smaller than that predicted by the diffusion model. If we use this as the cutoff point for the validity of the diffusion model, we can calculate a cutoff density (ρ_c) below which the hard-collision model must be used to predict the spectral line shape. These cutoff densities are given in Table III for all the Q-branch linewidths measured at temperatures of 81, 298, and 474 K. Note that ρ_c is approximately 1 amagat and varies only by a factor of 2 over this temperature range. In our fitting procedure, we only use linewidths for densities larger than ρ_c, and thus the temperature dependence of D_0 can be extracted from the A parameters given in Table I. The temperature dependence of D_0 is discussed in Sec. IV C below.

As the density further increases above 1 amagat (see Fig. 6), the linewidth is broadened, primarily due to inelastic rotational collisions (for Raman Q-branch transitions). This broadening is linearly dependent on density, and a Lorentzian line-shape results.

If the processes of collisional narrowing and density broadening are considered statistically independent, the total line shape is the convolution of two Lorentzians (assuming the diffusion model for collisional narrowing). Thus, the resulting Lorentzian line shape will have a width that is the sum of a term inversely proportional to density and one linearly dependent on density. This is the expression given in Eq. (1), used to model our measured Raman linewidths.

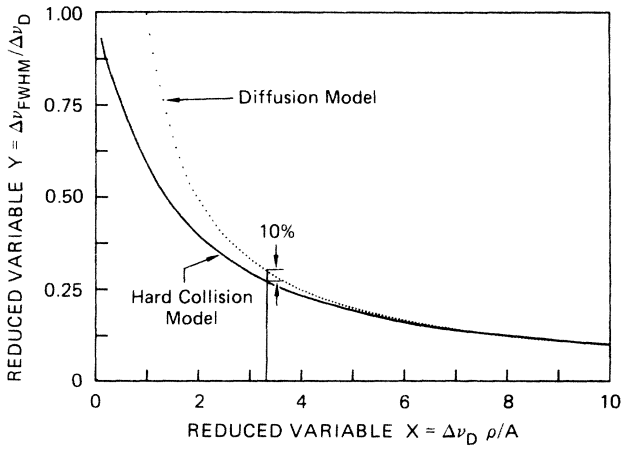

FIG. 7. Calculated collision narrowing of the FWHM Raman linewidths for the hard-collision model and the diffusion model (after Ref. 22). The hard-collision model predicts a linewidth that is 10% smaller than that predicted by the diffusion at $X=3.33$. This value of X is used to calculate the cutoff density ρ_c for the data analysis.

A. Temperature dependence of the Raman density-broadening coefficient

A good review of the relationship of Raman linebroadening coefficients to intermolecular forces is given by Srivastava and Zaidi.[30] In general, the collisional processes that contribute to the linewidths for isotropic Raman scattering (e.g., vibrational Q branch) are different from those that contribute to anisotropic Raman scattering (rotational S branch). Thus we obtain complementary information about the intermolecular forces by studying both the density and temperature dependence of both the rotational and vibrational Raman linewidths.

Hydrogen is a unique system in which to test linebroadening theories because the large rotational level spacing allows most of the population to be placed in one or two rotational levels at low temperatures. This can have important implications for the understanding of collisional contributions to the linewidth.

The first theoretical study of the vibrational Q-branch transition for H_2 was the work of Van Kranendonk.[3] This work has served as the basis for several extensions of the work to rotational Raman linewidths.[30–34] Table IV compares his calculated Q-branch linewidths for H_2 at room temperature with experimental measurements. Van Kranendonk obtained good agreement for all Q-branch transitions except the $Q(1)$ line, for which the theory gave a linewidth that was a factor of 3 too low. Another research group using his basic theory has obtained similar results,[8] also given in Table IV. There has been only one other study of Q-branch linewidths. Bonamy *et al.*[4] explicitly considered the temperature dependence of the Q-branch linewidths in HD. However, this theory has not yet been applied to the self-broadening of the Q-branch linewidths in H_2.

In general, the line-broadening coefficient has contributions from elastic collisions, which cause perturbations in the phase of the radiation field, and inelastic collisions, which remove the molecule from the rotational level involved in the radiation process. For the purposes of this discussion, the most important conclusions that have been reached by both Bonamy *et al.*[4] and Van Kranendonk[3] is that, in the absence of vibrational effects, the widths of the Q-branch lines are due exclusively to inelastic rotational collisions, and that the contribution of the elastic phase-perturbing collisions is identically zero. This is not the case for the rotational Raman lines; hence the linewidths of these transitions are generally larger than the Q-branch linewidths [see Fig. 4 for a comparison of the $Q(1)$ to the $S(1)$ linewidths].

The most important inelastic collision for H_2 is the resonant collision. An example of this type of collision is a radiating molecule in the $J_R=1$ level colliding with $J_p=3$ and exchanging rotational quantum numbers (resonant collisions between odd and even J's for H_2 and D_2 are forbidden by the ortho-para spin rule). Because the net energy exchange is zero, the temperature dependence of the resonant collision rate is proportional to the Boltzmann factor for the population in the $J=3$ level. All other inelastic collisions [such as $(J_R,J_p)=(1,2)\rightarrow(3,0)$ with $\Delta E=233\ \mathrm{cm}^{-1}$] are less probable, and

TABLE IV. Comparison between theory and experiment for the Q-branch Raman linewidths.

			$\Delta\nu$ (MHz/amagat)			
			Theory		Experiment	Vibrational contribution
T (K)	J	n_J	Ref. 3	Ref. 8	(this work)	(MHz/amagat)
81	0	0.25	<2	<2	29.0±1.0	29.0±1.0
	0	0.89	<2	<2	45.4±0.8	45.4±0.8
	1	0.75	<2	<2	41.5±0.6	41.5±0.6
298	0	0.130	66	78	77.0±1	0–9
	1	0.658	18	24	52.4±0.6	28–34
	2	0.117	78	86	80.0±11[a]	0–2±11
	3	0.090	108	116	137.0±28[a]	21–29±28

[a]Average of values in Refs. 6, 8, and 22.

hence have a smaller contribution to the linewidth.

Table IV shows that this model gives good agreement for all the Q-branch transitions except the $Q(1)$ line. A qualitative explanation for this discrepancy was first suggested by Allin *et al.*[6] and later by Gray and Welsh.[35] They suggested that the additional broadening for the $Q(1)$ line is connected with a vibrational perturbation mechanism that is proportional to the population in the initial state. This mechanism can be thought of as a vibrational dephasing contribution to the linewidth that arises from elastic collisions.[4] We therefore suggest a phenomenological model for the temperature dependence of the Q-branch linewidths as

$$B(J,T)=\alpha_i+\alpha_c n(J,T)+\beta(J,T,R_{\text{o-p}}) , \tag{8}$$

where B is the FWHM linewidth in MHz/amagat given in Table I, and $n(J,T)$ is the relative population in the J rotational level at temperature T. The $\alpha_{i,c}$ coefficients are contributions from vibrational dephasing, and the β coefficient results from rotationally inelastic collisions. The β coefficient depends on T, J, and the ortho-para ratio $R_{\text{o-p}}$ and has been calculated by Van Kranendonk[3] for $T=300$ K and $R_{\text{o-p}}=3$ (see Table IV). Since β in Eq. (8) is approximately zero at 81 K (see, for example, the analysis in Ref. 10), an analysis of the linewidths at low temperature will give the vibrational dephasing contribution to the linewidth.

Following the analysis in Ref. 11, $\alpha_i(T)$ is a temperature-dependent coefficient related to the isotropic molecular forces, whereas $\alpha_c(T)$ is the temperature-dependent coupling coefficient giving a linewidth proportional to the relative density in the J rotational level $n(J,T)$. Figure 8 gives our data at 81 K for both the $Q(0)$ and $Q(1)$ lines plotted as a function of relative density $n(J,T)$. The data are well fit by a straight line giving $\alpha_i=23$ MHz/amagat and $\alpha_c=25$ MHz/amagat. Although this result is encouraging, more data at different ortho-para ratios are needed to completely verify this analysis.

Using Eq. (8), we can determine the vibrational contribution to the linewidth at $T=298$ K by subtracting the calculated values of β given in Table IV from our data. The ranges of the residual contribution that can be attributed to vibrational dephasing are given in Table IV. This analysis is only qualitative and large uncertainties are presented in Table IV. However, we find that the available data at 298 K can be best represented by $\alpha_i=0\pm5$ and $\alpha_c=45\pm5$ MHz/amagat. A value of $\alpha_c=42$ MHz/amagat was proposed in Ref. 35. The values of $\alpha_{i,c}$ at 298 and 81 K are given in Table V and compared with values obtained for the line-shift coefficients. Again, more measurements are needed, particularly as a function of ortho-para ratios.

From this analysis, we conclude that the main contribution to the Raman linewidth at 81 K comes from vibrational dephasing collisions, an effect not included in any current theoretical analysis of the Q-branch linewidths of H_2. In addition, we conclude that over two-thirds of the $Q(1)$ linewidth comes from vibrational dephasing at $T=298$ K. These conclusions are, however, only qualitative at this point. New theoretical studies are needed to calculate the broadening coefficients as a function of temperature and to relate the $\alpha_{i,c}$ to specific intermolecular forces. With the present experimental techniques, we are able to accurately determine these very small density-broadening coefficients at low densities, thus providing new opportunities for theoretical studies of Raman linewidths.

B. Temperature dependence of the Raman line shift

In the only theoretical analysis of the Q-branch line-shift in H_2 as a function of temperature,[11] a statistical

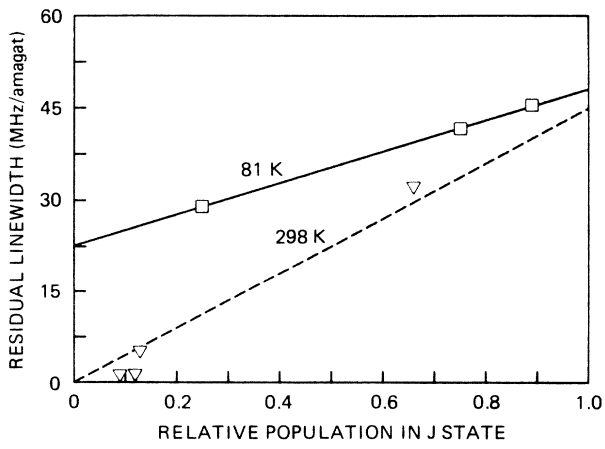

FIG. 8. Vibrational contribution to the Raman linewidth at 81 K (□) and 298 K (△). The solid and dashed lines are fits whose coefficients are listed in Table V.

TABLE V. Vibrational contribution to the Q-branch linewidth and line shift.

	Coefficients (MHz/amagat) Linewidth [Eq. (8)]					
	a_i			a_c		
T (K)	This work	Previous Expt.	Theory	This work	Previous Expt.	Theory
81	23±			25±1		
298	0±5			45±5	42[a]	
	Line shift [Eq. (9)]					
	a_i			a_c		
81	−225	−261[b]	−260[b]	−100	−42[b]	−63[b]
298	−58	−60[b]	−60[b]	−58	−51[b]	−63[b]
		−45[c]			−68[c]	

[a]Previously suggested in Ref. 35.
[b]Reference 11.
[c]Reference 7.

model for the vibrational perturbation of the transition frequency was used to derive the line shift from a Lennard-Jones potential model. In this analysis, the linear line shift parameter (C in Table II) could be divided into two parts (similar to the line-broadening discussion above):

$$C = a_i(T) + a_c(T) n(J,T) , \tag{9}$$

where a_i was interpreted in terms of the vibrational frequency perturbation arising from isotropic intermolecular forces, whereas a_c was shown to arise mainly from molecular coupling through the dispersion forces. It was found that a_i was strongly dependent on temperature, but a_c had only a small temperature dependence. A detailed discussion of the interpretation of a_i and a_c in terms of the intermolecular forces can be found in Refs. 11 and 35. The calculated values of a_i and a_c at 298 and 85 K are given in Table V along with values derived using Eq. (9) from our data in Table II and the experimental measurements of May *et al.*[11] and Lallemand and Simova.[7] The theory is in reasonable agreement with experiment. The theory also predicts that $C=0$ at $T\sim 393$ K, in approximate agreement with our finding, see Eq. (4), that $C=0$ at $T=446$.

However, there have been no line-shift calculations using a unified approach that simultaneously calculate the line-broadening coefficient. Although this has been done for HD by Bonamy *et al.*[4] using an impact theory, the theory has yet to be applied to H_2. The simultaneous calculation of the line shift and line broadening as a function of temperature and ortho-para ratio would be a stringent test of any impact theory. There appears to be a need for new theoretical advances in this area.

C. Temperature dependence of the diffusion coefficient

The final parameter that can be determined from the present measurement is the temperature dependence of the self-diffusion coefficient D_0 used in Eq. (7). There have been several determinations of the temperature dependence of this coefficient as discussed in Ref. 21, and a comparison of data and calculations is given in Ref. 36. There appears to be reasonable agreement between experiment and theory for temperatures above 65 K. Figure 9 plots the theoretical temperature dependence of D_0 for H_2 and shows that it follows a $T^{0.72}$ power law for temperatures above 65 K. Figure 9 also plots the values of D_0 determined at 81, 298, and 474 K from the Raman gain experiment (see Table III). For the $Q(1)$ transition at 298 and 81 K, the agreement is reasonably good, but there is marked disagreement at 474 K. The best power law that can be obtained for the three points is $T^{0.92}$. It may be that the coefficient determined from Raman linewidth data cannot be represented by a power law scaling at high temperatures.

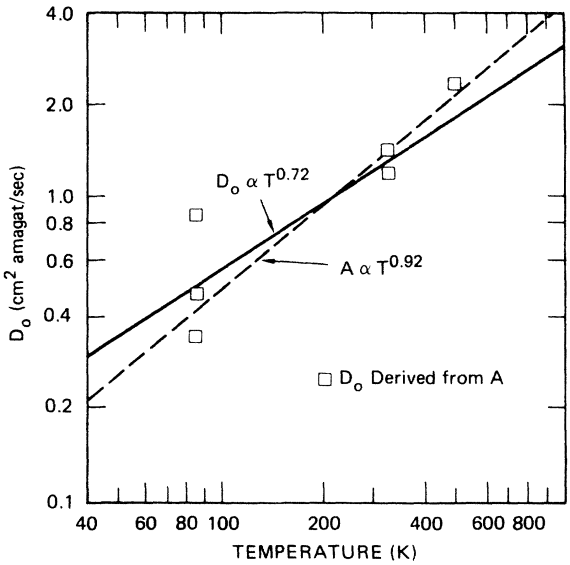

FIG. 9. Temperature dependence of the self-diffusion coefficient D_0. The solid line represents the theoretical and experimental values given in Ref. 36. The squares are values for D_0 determined from the Raman experiment (Table IV). The dashed line is the best fit for a power-law dependence for the $Q(1)$ transition.

In addition, we find that D_0 determined from the $Q(0)$ linewidth data are lower than for the $Q(1)$ data varying by a factor of 2.5 with respect to the ortho-para ratio at 81 K. Although there has been some discussion in the literature of quantum symmetry effects[37,38] that give different values of D_0 as a function of ortho-para ratios, these effects occur at temperatures below 40 K and hence cannot be used to explain the variations observed in this experiment. We, therefore, have no current explanation for the observed dependence of the A parameter, see Eq. (1), on temperature and ortho-para ratio.

V. SUMMARY AND CONCLUSION

We have measured the Raman linewidth and line-shift coefficients for the $Q(0)$ and $Q(1)$ vibrational transitions as a function of temperature for two ortho-para ratios. We conclude that the dominant contribution to the Raman linewidth at 81 K is due to vibrational dephasing collisions, and that at 298 K these collisions still result in over two-thirds of the observed linewidth for the $Q(1)$ transition. Because these effects are not included in any current theory of the Q-branch Raman linewidths, there is a need for new theoretical studies.

The observed Raman line shifts as a function of temperature for the $Q(0)$ and $Q(1)$ are in good agreement with previous measurements. The line-shift coefficient has a much larger temperature variation than the linewidth coefficient, with the ratio of line shift to linewidth reaching a maximum value of 7.3 at 81 K. The theoretical prediction that the linear coefficient of the density line shift for the $Q(1)$ transition should be zero at 393 K has been experimentally measured to occur at 446 K. There has been no theoretical study of the Q-branch Raman line shift in H_2 since 1964. The progress in both theoretical and experimental techniques since that time can now allow a detailed comparison between theory and experiment. Further progress on this problem requires new theoretical studies.

Finally, we conclude that the existing theory for the temperature dependence of the self-diffusion coefficient D_0 does not predict the dependence observed for the A parameter determined from the Raman linewidth measurements. Although there is reasonable agreement at 298 K, there is marked disagreement at 474 K and at 81 K, where we measure a dependence of A on ortho-para ratio. The fact that A changes by a factor of 2.5 when the ortho-para ratio goes from 3:1 to 1:7.7 cannot be explained by any current theory for D_0. We are led to the conclusion that the one-parameter diffusion model for the Raman line shape at densities above 1 amagat is not detailed enough to predict the temperature dependence of the collisionally narrowed Raman linewidth. It may be that the assumption of the statistical independence between the collisional narrowing of the Doppler width and the density broadening is not valid at low temperatures. Study of the ramifications of this change in assumptions is beyond the scope of this study, but should be theoretically addressed to direct new experimental efforts.

Note added in proof. In Sec. III B it was concluded that the $Q(1)$ Raman frequency was only known to an accuracy of 0.02 cm^{-1}. A recent comparison of high-resolution Fourier-transform Raman data (Ref. 39 and references therein) to ir absorption data indicates that the Q-branch transition frequencies are now known to better than 0.001 cm^{-1}.

ACKNOWLEDGMENTS

We thank D. L. Huestis for stimulating conversations and help with the data-fitting routines. We thank J. R. Murray for providing unpublished calculations of the hard-collision model necessary for Fig. 7. This work was supported by National Science Foundation (NSF) Engineering Grant No. ECS-8213373 and by the Defense Advanced Research Projects Agency under Contract No. N00014-80-C-0506, through the U.S. Office of Naval Research. We acknowledge the use of a Digital Equipment Corporation VAX 750 computer system purchased under NSF Grant No. PHY-8114611.

[1]Adelbert Owyoung, in *Chemical Applications of Nonlinear Raman Spectroscopy,* edited by Albert B. Harvey (Academic, New York, 1981), pp. 281–320; Peter Esherick and Adelbert Owyoung, in *Advances in Infrared and Raman Spectroscopy,* edited by R. J. H. Clark and R. E. Hestor (Heyden, London, 1983), Vol. 9.

[2]R. P. Srivastava and H. R. Zaidi, in *Raman Spectroscopy of Gases and Liquids,* edited by A. Weber (Springer-Verlag, Berlin, 1979), pp. 167–198.

[3]J. Van Kranendonk, Can. J. Phys. **41**, 433 (1963).

[4]Jeanine Bonamy, Lionel Bonamy, and Daniel Robert, J. Chem. Phys. **67**, 4441 (1977).

[5]J. V. Foltz, D. H. Rank, and T. A. Wiggins, J. Mol. Spectrosc. **21**, 208 (1966).

[6]Elizabeth J. Allin, A. D. May, B. P. Stoicheff, J. C. Stryland, and H. L. Welsh, Appl. Opt. **6**, 1597 (1967).

[7]P. Lallemand and P. Simova, J. Mol. Spectrosc. **26**, 262 (1968).

[8]R. H. Hunt, W. L. Barnes, and P. J. Brannon, Phys. Rev. A **1**, 1570 (1970); P. J. Brannon, J. Quant. Spectrosc. Radiat. Transfer **8**, 1615 (1968).

[9]Adelbert Owyoung, Opt. Lett. **2**, 91 (1978).

[10]K. D. van den Hout, P. W. Hermans, E. Mazur, and H. F. P. Knaap, Physica **104A**, 509 (1980).

[11]A. D. May, G. Varghese, J. C. Stryland, and H. L. Welsh, Can. J. Phys. **42**, 1058 (1964); E. C. Looi, J. C. Stryland, and H. L. Welsh, *ibid.* **56**, 1102 (1978).

[12]H. Komine and E. A. Stappaerts, Opt. Lett. **7**, 157 (1982).

[13]C. Woods, K. Tang, C. Howton, D. Muller, and R. O. Hunter, Jr., in *Excimer Lasers—1983,* edited by C. K. Rhodes, H. Egger, and H. Pummer (AIP, New York, 1983).

[14]R. S. F. Chang and N. Djeu, Opt. Lett. **8**, 139 (1983).

[15]V. Wilke and W. Schmidt, Appl. Phys. **18**, 177 (1979); **16**, 151 (1978).

[16]D. J. Brink and D. Proch, Opt. Lett. **7**, 494 (1982).

[17]H. F. Döbele, M. Röwekamp, and B. Rückle, IEEE J. Quantum Electron. **QE-20**, 1284 (1984).

[18]A. P. Hickman, J. A. Paisner, and William K. Bischel, Phys. Rev. A **33**, 1788 (1986).
[19]W. K. Bischel and M. J. Dyer, in *Excimer Lasers—83*, edited by C. K. Rhodes, H. Egger, and H. Pummer (AIP, New York, 1983).
[20]W. R. Trutna and R. L. Byer, Appl. Opt. **19**, 301 (1980).
[21]Joseph O. Hirschfelder, Charles F. Curtiss, and R. Byron Bird, *Molecular Theory of Gases and Liquids* (Wiley, New York, 1954).
[22]J. R. Murray and A. Javan, J. Mol. Spectrosc. **42**, 1 (1972).
[23]G. H. Rosasco, W. S. Hurst, and W. Lempert, Opt. Lett. **9**, 19 (1984).
[24]B. P. Stoicheff, Can. J. Phys. **35**, 730 (1957).
[25]P. J. Brannon, C. H. Church, and C. W. Peters, J. Mol. Spectrosc. **27**, 44 (1968).
[26]R. H. Dicke, Phys. Rev. **89**, 472 (1953).
[27]S. G. Rautian and I. I. Sobel'man, Usp. Fiz. Nauk **90**, 209 (1966) [Sov. Phys.—Usp. **9**, 701 (1967)].
[28]Joel I. Gersten and Henry M. Foley, J. Opt. Soc. Am. **58**, 933 (1968).
[29]Louis Galatry, Phys. Rev. **122**, 1218 (1961).
[30]R. P. Srivastava and H. R. Zaidi, Can. J. Phys. **55**, 542 (1977).
[31]C. G. Gray and J. Van Kranendonk, Can. J. Phys. **44**, 2411 (1966).
[32]H. Moraal, Physica **73**, 379 (1974).
[33]D. Robert and J. Bonamy, J. Phys. (Paris) **40**, 923 (1979).
[34]D. A. Coombe and W. E. Kohler, Physica **100A**, 453 (1980); **100A**, 472 (1980).
[35]C. G. Gray and H. L. Welsh, in *Essays in Structural Chemistry*, edited by A. J. Downs, D. A. Long, and L. A. K. Staveley (Macmillan, London, 1971), p. 163.
[36]I. Amdur and J. W. Beatty, Jr., J. Chem. Phys. **42**, 3361 (1965).
[37]A. Hartland and M. Lipsicas, Phys. Lett. **3**, 212 (1963).
[38]E. G. D. Cohen, M. J. Offerhaus, J. M. M. Van Leeuwen, B. W. Roos, and J. De Boer, Physica **22**, 791 (1956).
[39]D. E. Jennings, A. Weber, and J. W. Brault, Appl. Opt. **25**, 284 (1986).